

Experimental study of K-shell X-ray emission generated from nanowire target irradiated by relativistic laser pulses

Ye Tian (田野), Wentao Wang (王文涛)*, Cheng Wang (王成), Xiaoming Lu (陆效明),
Cheng Wang (王乘), Yuxin Leng (冷雨欣), Xiaoyan Liang (梁晓燕), Jiansheng Liu (刘建胜)**,
Ruxin Li (李儒新), and Zhizhan Xu (徐至展)

Shanghai Institute of Optics and Fine Mechanics, Chinese Academy of Sciences, Shanghai 201800, China

*Corresponding author: wwt1980@yeah.net; **corresponding author: michaeljs_liu@mail.siom.ac.cn

Received July 16, 2012; accepted October 10, 2012; posted online January 30, 2013

K-shell X-ray emission from a Cu nanowire target irradiated by an ultraintense femtosecond laser pulse is studied using an elliptically bent quartz crystal and imaging plate. The designed bent crystal spectrometer has better spectral resolution, which is higher than 1000. The absolute $K\alpha$ radiation photon yields are obtained from the experimental results and the Monte-Carlo model. The conversion efficiency of the Cu $K\alpha$ line is estimated to be 0.019% from the interaction of 4 J, 50-fs laser pulse irradiated on a Cu nanowire target. The high yield of K shell X-ray has important applications in X-ray emission source.

OCIS codes: 300.6560, 350.5400, 350.5610.

doi: 10.3788/COL201311.033501.

X-ray emission is a powerful diagnostic tool in many fields, including biomedical imaging^[1] and X-ray diffraction^[2]. In particular, with the development of ultrashort ultraintense laser technology, short pulse (<1 ps) laser-matter interaction has attracted great interest owing to its applications in fast ignition diagnostics^[3] and X-ray backlighters^[4]. X-ray bremsstrahlung and characteristic inner-shell line emissions, which come from the K-shell, are produced when laser-induced energetic electrons propagate into the bulk of a solid target^[5]. Several tools have been developed to detect intense X-ray radiation. One of these is the Bragg bent crystal, which is one of the routine tools used in keV X-ray imaging and spectra^[6]. A high-quality crystal surface structure can obtain a backlight source image using optical-contact fabrication techniques. Recently, the development of the record medium, including the X-ray charge coupled device (CCD), imaging plate (IP), and X-ray films, has greatly promoted X-ray measurement^[7]. Another detecting medium IP (Fuji BAS series), which has already shown great performance in high energy electron research, is applied in X-ray detection; its advantages include higher dynamic range and greater sensitivity than X-ray films in several keV ranges. Luo *et al.*^[8] tested the IP response curve line to X-ray from 10 to 60 keV, and their result agrees well with the Monte Carlo N2 particle transport code (MCNP) simulation results.

Intense picosecond X-ray has been obtained by irradiating a nanowire material with 1 ps pulses at an intensity of 10^{17} W/cm², producing ps soft X-ray pulses that are 50 times more efficient than solid targets^[9]. Through experiments and simulations, recent studies have conducted in-depth investigations of the X-ray sources obtained from the respective interactions between laser and different solid targets (Z from 10 to 80), gas, or nanowire materials^[10–14]. A more efficient laser energy absorption leads to intense interactions that, in turn, produce greater doses of X-ray emission. This is due to the $K\alpha$ radiation generated by the inner-shell ionization of the

target atoms, and the successive radioactive decay of the atom in the excited state, which is relevant to the energy deposition of the relativistic electron. Nevertheless, further investigations on spectra and absolute yields of photons are still required to help us gain a better understanding of the fundamental mechanism of relativistic electron transport dynamics.

The experiment was carried out using the petawatt laser facility at the Shanghai Institute of Optics and Fine Mechanics (SIOM). The laser system provides a p-polarized pulse with single-shot energy, which fluctuates from 4 to 5 J in 50 fs at 800 nm. The amplified spontaneous emission was measured to be $\sim 10^{-6}$. The laser pulse was focused with a $f/10$ off-axis parabolic mirror onto a Cu nanowire target. The total thickness of the surface was about 10 μm , the nanowire length was about 9 μm , and the nanowire diameter ranged from 300 to 500 nm (Fig. 1).

The diameter of the focal spot was 20 μm at full width half maximum (FWHM). The schematic of the experiment setup is shown in Fig. 1. In the experiment, the laser pulse irradiated the target with a 45° incident angle at an intensity of up to 1×10^{19} W/cm². An elliptical quartz bent crystal was used in detecting the X-ray spectra emitted by the laser-produced plasma. The focal length of the crystal was 630 mm with elliptical eccen-

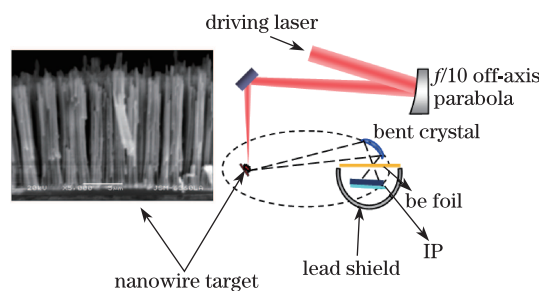


Fig. 1. Schematic diagram of the experimental setup and SEM image of the Cu nanowire target.

tricity $\varepsilon=0.945$. Elliptical bent crystal was aligned by laser diode (LD) in order to maintain an accurate angle and distance between the focal spot and the detector, thereby satisfying the elliptical equation for the imaging condition. In the Bragg equation $2d \sin \theta = n \lambda$, $2d$ is the lattice constant, θ is the incident angle, and λ is the reflected X-ray wavelength. The quartz crystal lattice constant is 0.2749 nm; thus, the detecting range is from 0.153 nm to 0.155 nm, where the Cu $K\alpha$ spectrum is located. A piece of Be foil with thickness of 25 μm was used as a filter in front of the IPs in order to block out the background scattering light and X-ray with energy lower than 1 keV. Lead shield was placed around the IP to protect it against the background X-ray (Fig. 1). The exposed IPs were read using Fuji IP scanner (FLA7000) with the following settings: sensitivity (4000), latitude (5), scanning resolution (50 μm). The PSL signal level relates to the gray scale level in the digital image.

The single shot space-resolved spectrum of Cu $K\alpha$ line around 8 keV was recorded by the IP, which was obtained from the irradiation of the Cu nanowire target (Fig. 2). As can be seen, two emission line spectra are perpendicular to the spectrum divergence direction originating from front surface; however, the line is not continuous because of the crystal defects. The double line structures of the Cu $K\alpha$ lines shown in Fig. 2 are $K\alpha_1$ (0.15406 nm) and $K\alpha_2$ (0.15444 nm), respectively. The integrated peak intensity ratios of $K\alpha_1$ and $K\alpha_2$ both satisfy $I\alpha_1/I\alpha_2 \sim 2$, which agrees with previously reported results^[15]. Still in the raw dispersion spectrum, no continuous radiation is obtained (Fig. 2). In addition, the background noise signal mainly comes from high-energy charged particles

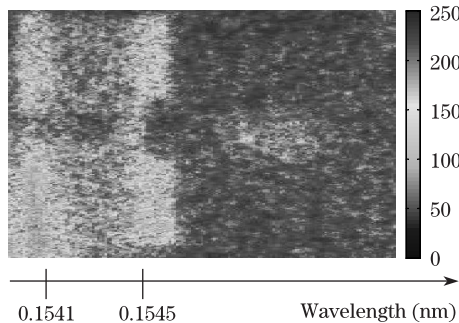


Fig. 2. Raw data of the $K\alpha$ line of Cu recorded by IP (10^{-1} nm/angstrom).

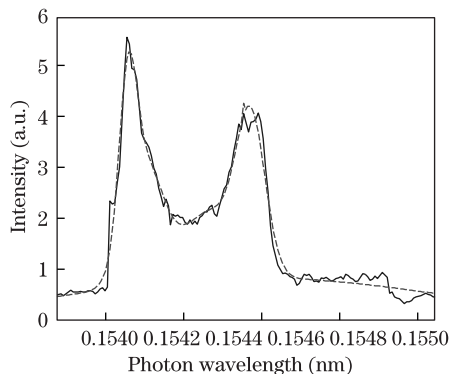


Fig. 3. X-ray emission spectrum around the $K\alpha$ line of Cu from the irradiation of a nanowire target at an intensity of 1×10^{19} W/cm².

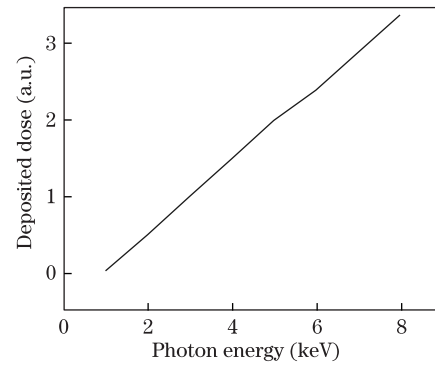


Fig. 4. X-ray deposition dose on the IP from 1 to 10 keV as simulated by EGSNRC.

and the effect of X-ray impacting on the IP.

The space-resolved spectrum of $K\alpha$ line along the dispersive direction is plotted in Fig. 3, which shows that the intensity is integrated within a 6-mm width sample box in the vertical direction. A Gaussian function is applied on the $K\alpha$ line to determine the spectral resolution of the elliptical bent crystal. The FWHM of the Gaussian function is $\sim 1 \times 10^{-4}$ nm, so the spectral resolution of the spectrometer in the experiment is better than 1000 (Fig. 3). The line spectra of X-ray around 8 keV represents a monochrome X-ray source, which has various applications in many fields.

In order to achieve the number of photons at 8 keV, the MCNP simulation program was employed to simulate the photon energy deposition in the IP. The parameters applied are according to the IP type (BAS-MS) used in the experiment. The IP consisted of a 9- μm protective layer made of PET and a 115- μm fluorescence layer consisting of a BaFX: Eu²⁺ and polyurethane compound. The energy deposited in the fluorescence layer of IP was read by He-Ne laser during the readout process. Concerning the thickness of the IP itself, the photons at different depths may either be scattered or absorbed. Thus, the fluorescence layer was divided into layers, and the attenuation model was applied in the simulation condition^[8].

The photon energy response curve of the IP was calculated. The results are shown in Fig. 4. At around 1 to 10 keV, the photon energy-deposited efficiency shows a linear relation between the deposited energy and the photon energy.

Three methods to test the instrument response to X-ray (i.e., X-ray films, X-ray CCDs, and IPs) were compared in the current work based on the experimental results of Howe *et al.*^[7]. At around 2 keV, the IP counts (PSL) and photon relationship are as follows: 1 PSL stands for 200 ± 50 photons. According to the data in Fig. 3, there exists a relationship between IP counts and photon number from 2 to 8 keV; specifically, a general relationship around 8 keV is represented by 1 PSL, which equals 25 ± 6 photons.

In the experiment, we scanned every IP for about 10 min after exposure. Considering the fading effect studied by Meadowcroft *et al.*^[16], the equation of the final signal relative to the original dose is given as

$$I(t) \approx 0.231 \exp[-(t/107)] + 0.779. \quad (1)$$

Thus, the signal level decreases to about 98% relative

to the original dose. The Cu $K\alpha$ yield is integrated in the range of FWHM centered at the $K\alpha_1$ line along the dispersive direction (i.e., in the vertical direction within a 6-mm width sample box shown in Fig. 3). In addition, the number of total X-ray photons is about 4200. The Be foil filter transmission is 99% (we did not consider target absorption). The receiving solid angle is 1.54×10^{-5} sr, and the transmission efficiency of the bent crystal is about 0.1^[17]. Thus, the total space Cu $K\alpha$ photons is about 4.5×10^{10} , corresponding to 0.76×10^{-4} J. Given that the total laser energy used is about 4 J, about 0.019% of the laser energy is transferred to the $K\alpha$ X-ray emission. A comparison between Cu solid target and nanowire target should be conducted in future works so as to identify direct evidence of the increased X-ray yield. The efficiency of the $K\alpha$ X-ray emission from irritating nanowire increased by approximately 10 times compared with the traditional solid or cluster targets^[4,18]. The high absorption of laser energy in the nanowire target and the strong interaction between the laser and target should be the reason for high $K\alpha$ photon yields^[14].

In conclusion, we present the K -shell X-ray emission from irradiating the nanowire target by laser pulse with peak focus intensity of approximately 1×10^{19} W/cm². We employ elliptical quartz bent crystal in order to detect Cu $K\alpha$ fine-structure spectra. Typically, the designed bent crystal spectrometer has a high spectral resolution, which is better than 1000. The total flux of K -shell photons reaches 3.4×10^{10} , and the conversion efficiency is 1.9×10^{-4} . The high yield of K shell X-ray has important applications in identifying X-ray emission source.

This work was supported by the National Basic Research Program of China (Nos. 011CB808100 and 2010CB923203), the National Natural Science Foundation of China (Nos. 10974214 and 60921004), the Shanghai Science and Technology Talent Project (No. 12XD1405200), and the State Key Laboratory Program of Chinese Ministry of Science and Technology. Finally, we would like to thank Professors S. L. Xiao and R. R. Wang for their suggestion to use the bent crystal design.

References

1. W. Li, S. Schulman, R. J. Dutton, D. Boyd, J. Beckwith, and T. A. Rapoport, *Nature* **463**, 507 (2010).
2. M. Bargheer, N. Zhavoronkov, Y. Gritsal, J. C. Woo, D. S. Kim, M. Woerner, and T. Elsaesser, *Science* **306**, 1771 (2004).
3. R. Kodama, K. A. Tanaka, Y. Sentoku, T. Matsushita, K. Takahashi, H. Fujita, Y. Kitagawa, Y. Kato, T. Yamanaka, and K. Mima, *Phys. Rev. Lett.* **84**, 4 (2000).
4. A. Lévy, F. Dorchies, P. Audebert, J. Chalupsky, V. Hájková, L. Juha, T. Kaempfer, H. Sinn, I. Uschmann, L. Vyšín, and J. Gaudin, *Appl. Phys. Lett.* **96**, 151114 (2010).
5. T. Brabec, *Strong Field Laser Physics* (Springer, Berlin, 2008).
6. S. Xiao, H. Wang, J. Shi, C. Tang, and S. Liu, *Chin. Opt. Lett.* **7**, 1 (2009).
7. J. Howe, D. M. Chambers, C. Courtois, E. Forster, C. D. Gregory, I. M. Hall, O. Renner, I. Uschmann, and N. C. Woolsey, *Rev. Sci. Instrum.* **77**, 036105 (2006).
8. Z. Luo, C. Suzuki, T. Kosako, and J. Ma, *Atomic Energy Science and Technology* (in Chinese) **7**, 43 (2009).
9. G. Kulcsár, D. AlMawlawi, F. W. Budnik, P. R. Herman, M. Moskovits, L. Zhao, and R. S. Marjoribanks, *Phys. Rev. Lett.* **84**, 5149 (2000).
10. H.-S. Park, D. M. Chambers, H.-K. Chung, R. J. Clarke, R. Eagleton, E. Giraldez, T. Goldsack, R. Heathcote, N. Izumi, M. H. Key, J. A. King, J. A. Koch, O. L. Anden, A. Nikroo, P. K. Patel, D. F. Price, B. A. Remington, H. F. Robey, R. A. Snavely, D. A. Steinman, R. B. Stephens, C. Stoeckl, M. Storm, M. Tabak, W. Theobald, R. P. J. Town, J. E. Wickersham, and B. B. Zhang, *Phys. Plasmas* **13**, 056309 (2006).
11. L. M. Chen, F. Liu, W. M. Wang, M. Kando, J. Y. Mao, L. Zhang, J. L. Ma, Y. T. Li, S. V. Bulanov, T. Tajima, Y. Kato, Z. M. Sheng, Z. Y. Wei, and J. Zhang, *Phys. Rev. Lett.* **104**, 215004 (2010).
12. N. Zhavoronkov, Y. Gritsai, G. Korn, and T. Elsaesser, *Appl. Phys. B* **79**, 663 (2004).
13. N. Zhavoronkov, Y. Gritsai, M. Bargheer, M. Woerner, T. Elsaesser, F. Zamponi, I. Uschmann, and E. Förster, *Opt. Lett.* **30**, 13 (2005).
14. L. Cao, Y. Gu, Z. Zhao, L. Cao, W. Huang, W. Zhou, X. T. He, W. Yu, and M. Y. Yu, *Phys. Plasmas* **17**, 043103 (2010).
15. P. Köster, K. Akli, D. Batani, D. Batani, S. Baton, R. G. Evans, A. Giulietti, D. Giulietti, L. A. Gizzi, J. S. Green, M. Koenig, L. Lbate, A. Morace, P. Norreys, F. Perez, J. Waugh, N. Woolsey, and K. L. Lancaster, *Plasma Phys. Control. Fusion* **51**, 014007 (2009).
16. A. L. Meadowcroft, C. D. Bentley, and E. N. Stott, *Rev. Sci. Instrum.* **79**, 113102 (2008).
17. B. L. Henke, P. Lee, and T. J. Tanka, *Atomic Data and Nuclear Data Tables* **27**, 1 (1982).
18. F. Liu, L.-M. Chen, X.-X. Lin, F. Liu, J.-L. Ma, R.-Z. Li, Y.-T. Li, Z.-H. Wang, S.-J. Wang, Z.-Y. Wei, and J. Zhang, *Opt. Express* **17**, 19 (2009).